

SUPPORTING INFORMATION

Superabsorbent cryogels decorated with silver nanoparticles as a novel water technology for point-of-use disinfection

Siew-Leng Loo^{†,‡}, Anthony G. Fane^{†,‡}, Teik-Thye Lim^{†,‡,*}, William B. Krantz^{†,§},
Yen-Nan Liang[¶], Xin Liu^{†,‡}, Xiao Hu^{†,¶*}

[†]Singapore Membrane Technology Centre, Nanyang Technological University, 1 Cleantech Loop, CleanTech One, #05-05, Singapore 637141, Singapore.

[‡]School of Civil and Environmental Engineering, Nanyang Technological University, Block N1, 50 Nanyang Avenue, Singapore 639798, Singapore.

[§]Department of Chemical and Biological Engineering, University of Colorado, Boulder, Colorado 80309-0424, USA.

[¶]School of Materials Science and Engineering, Nanyang Technological University, Singapore 639798, Singapore.

*Corresponding author: Tel.: +65 67906933; Fax: +65 67910676; Email: cttlim@ntu.edu.sg

**Corresponding author at: School of Materials Science and Engineering, Nanyang Technological University, Singapore 639798, Singapore. Tel: +65 67904610; Fax: +65 68909081; Email: ASXHU@ntu.edu.sg

The following is a list of additional supporting materials for the article:

- Fig. S1 Ag and Na concentration profiles during the Ag loading step of the intermatrix synthesis of AgNC-20
- Fig. S2 UV-visible absorption spectra of PSA/Ag cryogels with different Ag loadings. The inset shows the photographs of the as-synthesized cryogel nanocomposites.
- Fig. S3 FESEM images of (a) PSA cryogels, (b) AgNC-20, (c) AgNC-90 (the insets show the corresponding high-magnification images); EDX spectra of (d) PSA cryogel, and (e) AgNC-170.
- Fig. S4 Photographs taken during the compression tests of the PSA/Ag cryogel.
- Fig. S5 Disinfection efficacies of AgNC-170 (in the presence of quenching agent) as a function of contact time. The inset shows the corresponding total dissolved Ag and total Ag concentration in the squeezed water after the disinfection tests.

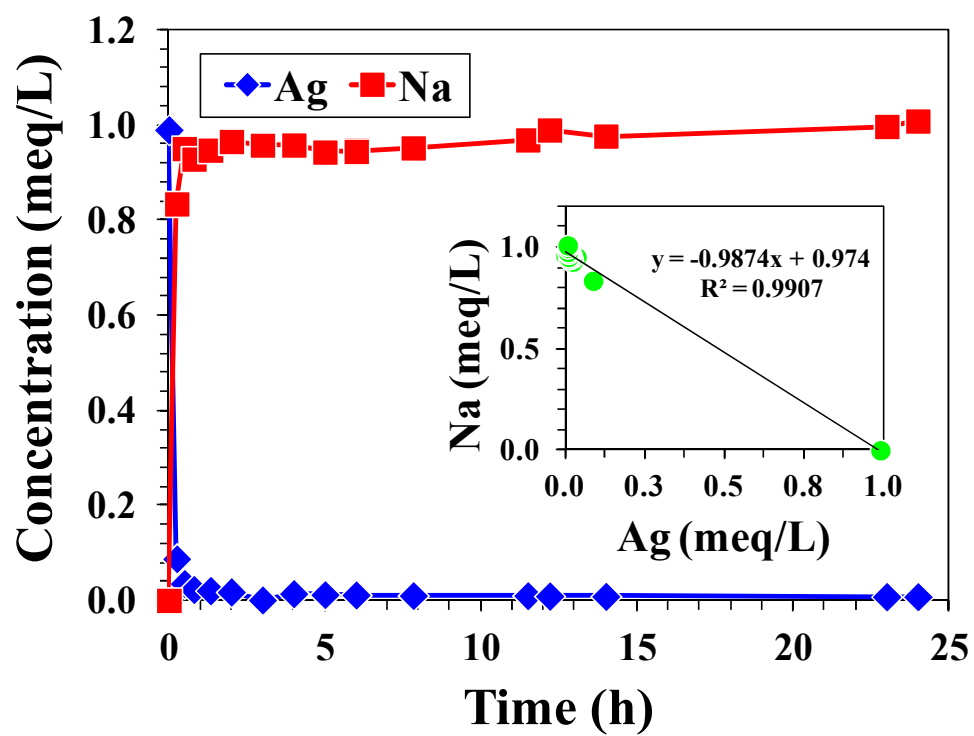


Fig. S1 Ag and Na concentration profiles during the Ag loading step of the intermatrix synthesis of AgNC-20.

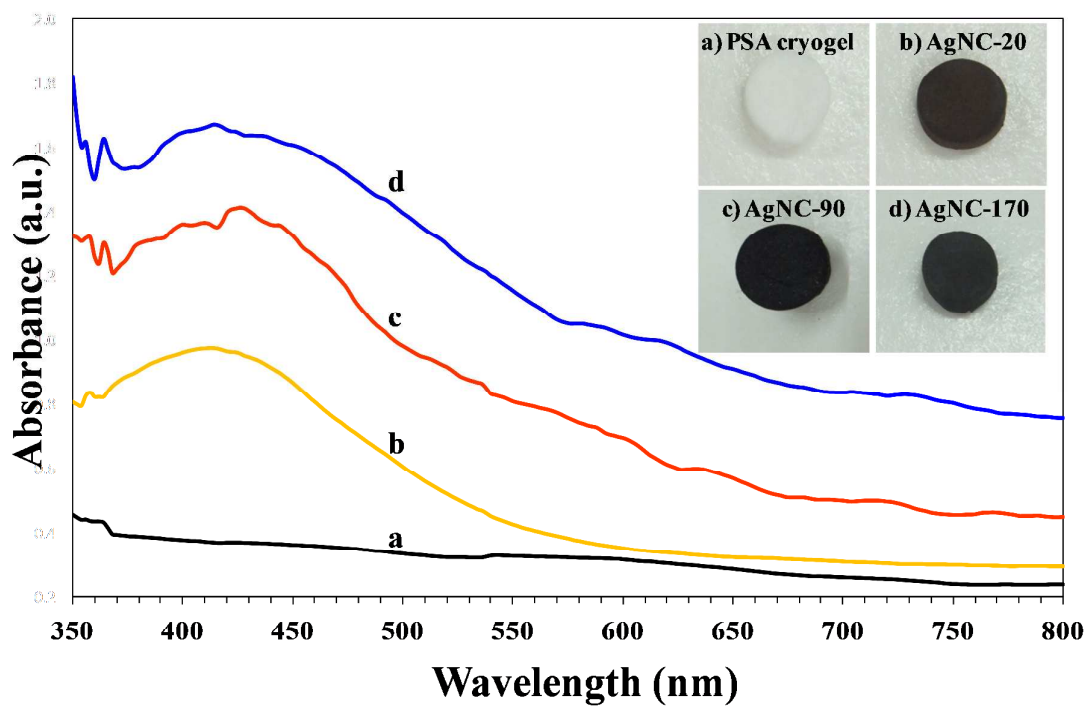


Fig. S2 UV-visible absorption spectra of PSA/Ag cryogels with different Ag loadings. The inset shows the photographs of the as-synthesized cryogel nanocomposites.

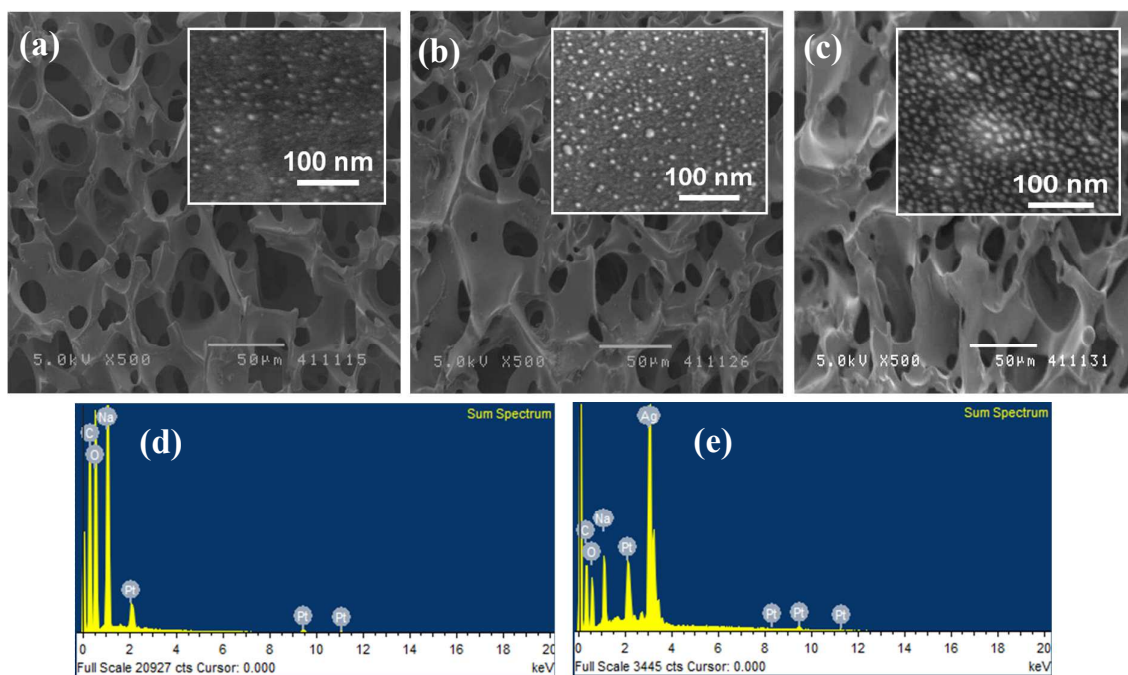


Fig. S3 FESEM images of (a) PSA cryogels, (b) AgNC-20, (c) AgNC-90 (the insets show the corresponding high-magnification images); EDX spectra of (d) PSA cryogel, and (e) AgNC-170.

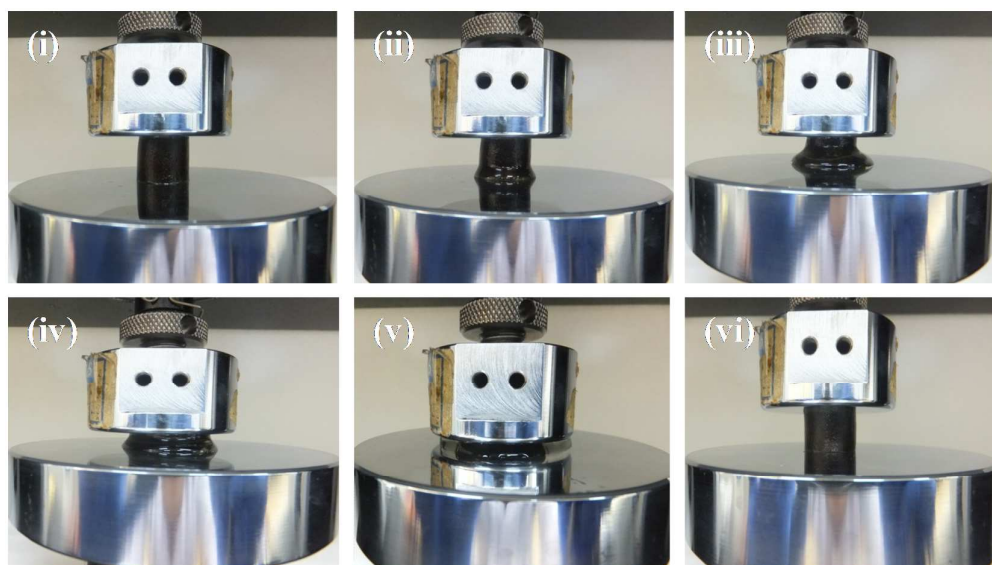


Fig. S4 Photographs taken during the compression tests of the PSA/Ag cryogel.

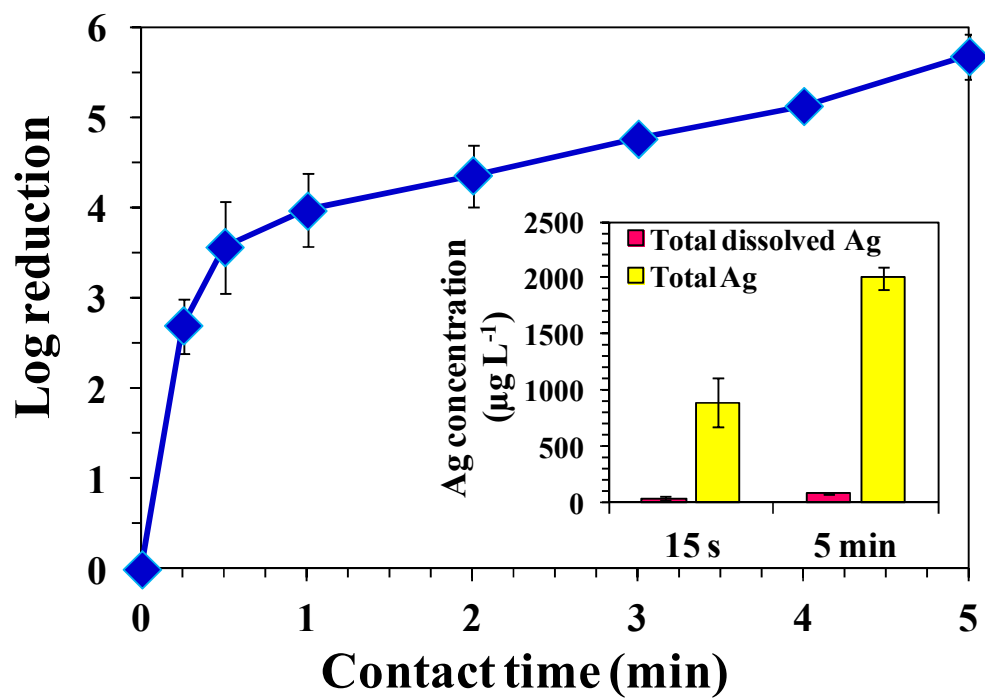


Fig. S5 Disinfection efficacies of AgNC-170 (in the presence of quenching agent) as a function of contact time. The inset shows the corresponding total dissolved Ag and total Ag concentration in the squeezed water after the disinfection tests.